Attribution of southern hemisphere climate change and projections

Meelis J. Zidikheri[1], Jorgen S. Frederiksen[2], and Carsten S. Frederiksen[1]

Centre for Australian Weather and Climate Research
Bureau of Meteorology[1]
CSIRO Marine and Atmospheric Research[2]

April 8, 2011

Table of contents

Introduction: Circulation changes

Introduction: Storm track changes

Introduction: Simulations

Introduction: Projections

Introduction: Attribution by model inversion

Two-level quasigeostrophic potential vorticity equations

Iterative method

Statistical dynamical method: Closure problem

Statistical dynamical method: Parameterisation

Statistical dynamical method: Closed form

Results: Linear regression of ensemble data points (1)

Results: Linear regression of ensemble data points (2)

Results: Forcing function anomalies compared

Summary and Conclusion

References

Introduction: Circulation changes

- Large changes in circulation patterns observed over late half of 20th Century
- In the southern hemisphere polar shift of the jet stream observed in winter

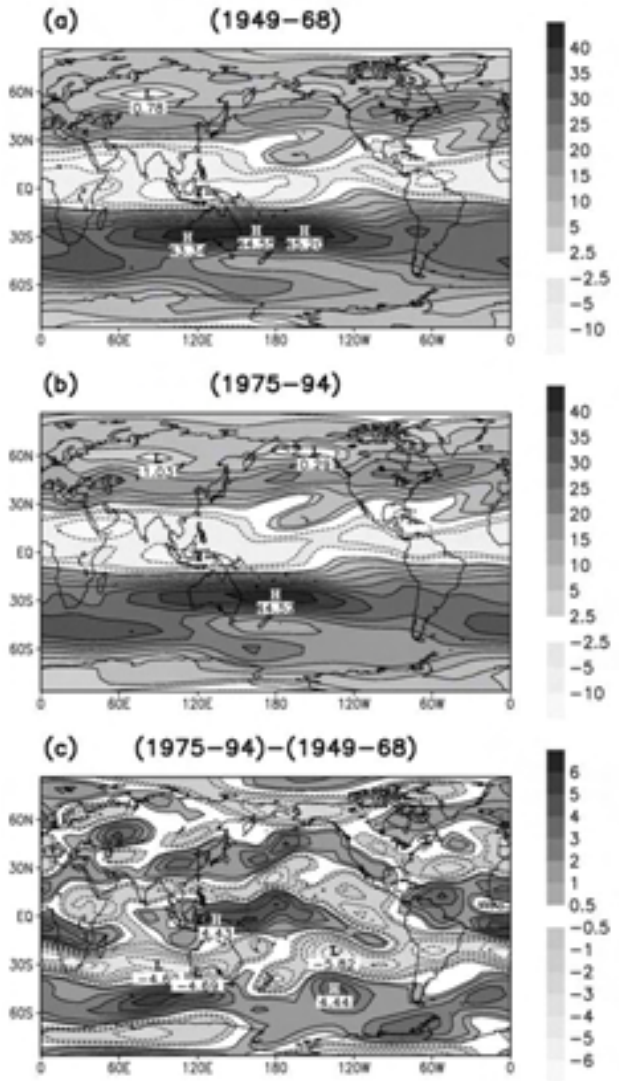

Figure: 300 hPa zonal velocity (m s^{-1}) from NCEP reanalysis for July.

Introduction: Storm track changes

- Changes in circulation patterns associated with changes in storm tracks
- Phillips instability criterion relates wind patterns to storm tracks

$$p = \langle u^{300} \rangle - \langle u^{700} \rangle - c \langle \sigma \rangle \frac{cos\phi}{\sin^2 \phi}$$

- Instability occurs when $p \geq 0$

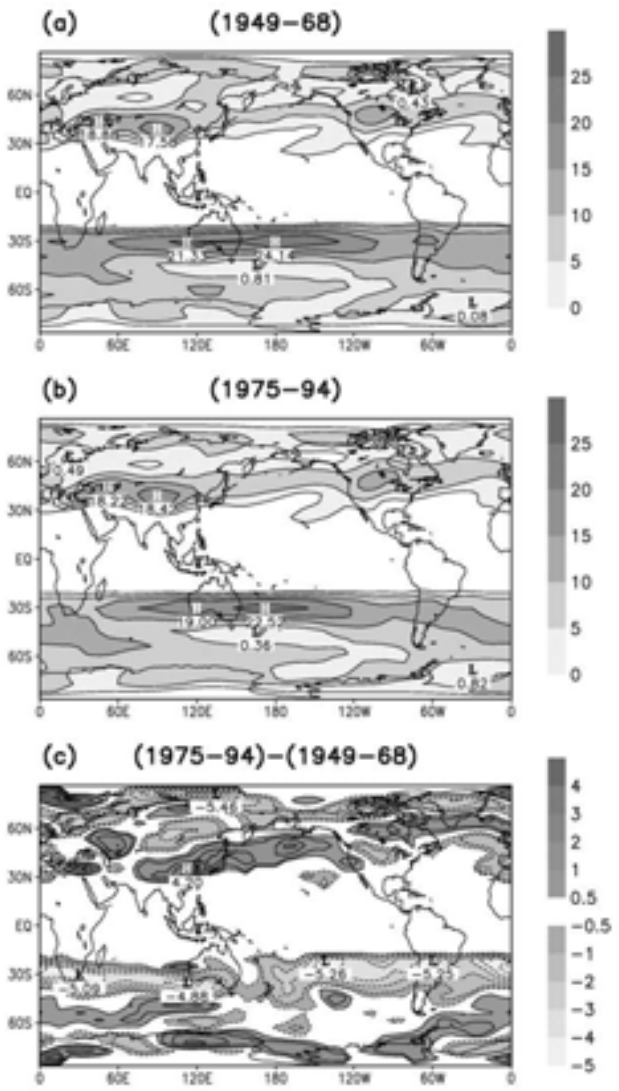

Figure: Phillips instability criterion (m s^{-1}) from NCEP reanalysis for July.

Introduction: Simulations

- Observed changes can be simulated well by some models

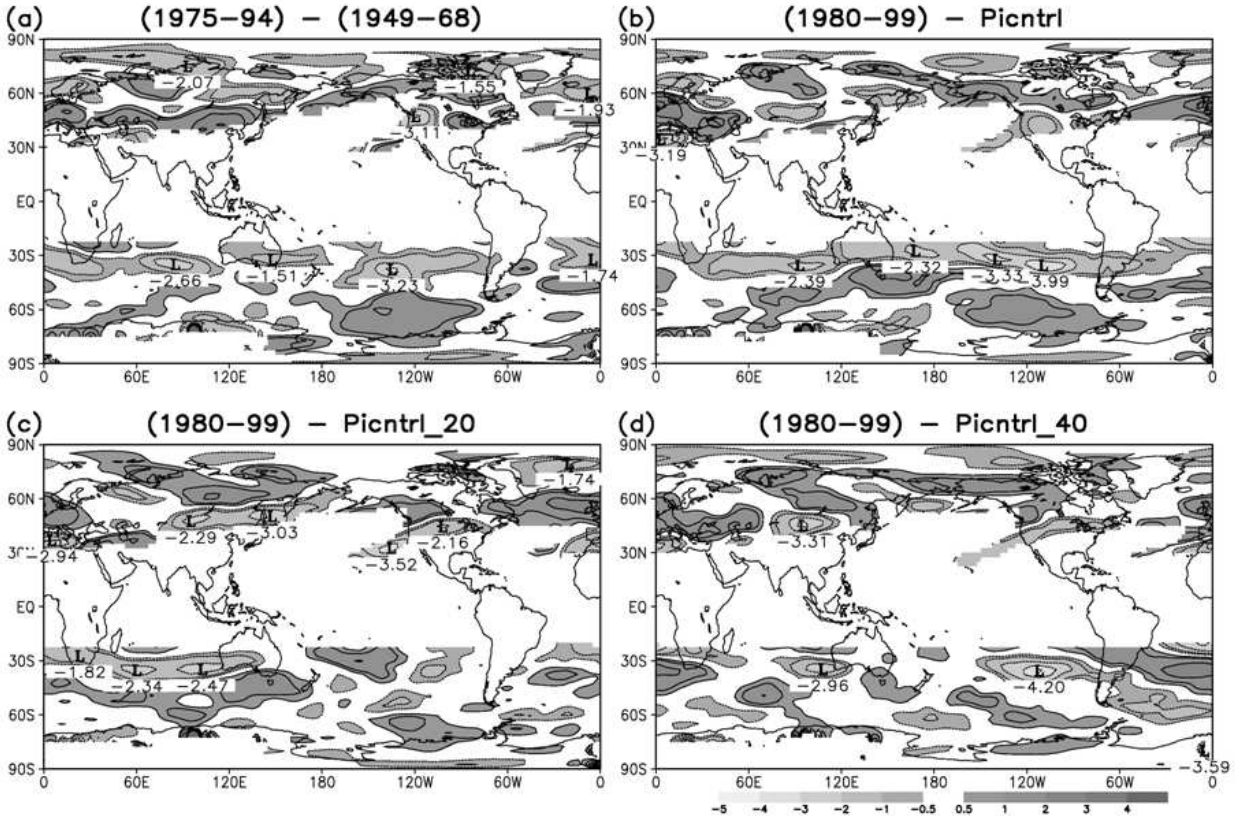

Figure: Phillips instability criterion changes (m s^{-1}) for July (observations and simulations compared).

Introduction: Projections

- Models predict further changes in storm tracks under different emission scenarios

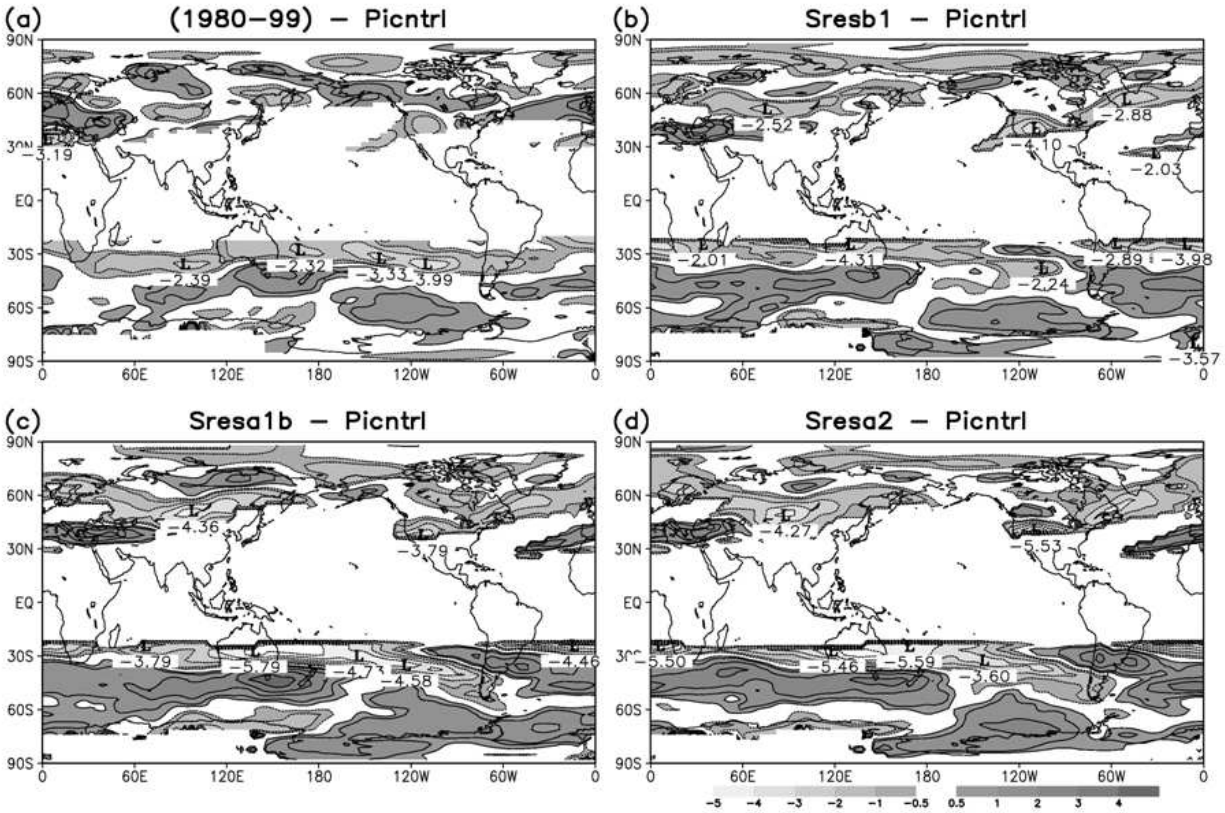

Figure: Phillips instability criterion changes (m s^{-1}) for July as projected under different emission scenarios.

Introduction: Attribution by model inversion

- It is possible to identify climate change drivers by directly inverting a climate model
- Geographical patterns of climate anomalies in general different to forcing function anomalies (climate change drivers)

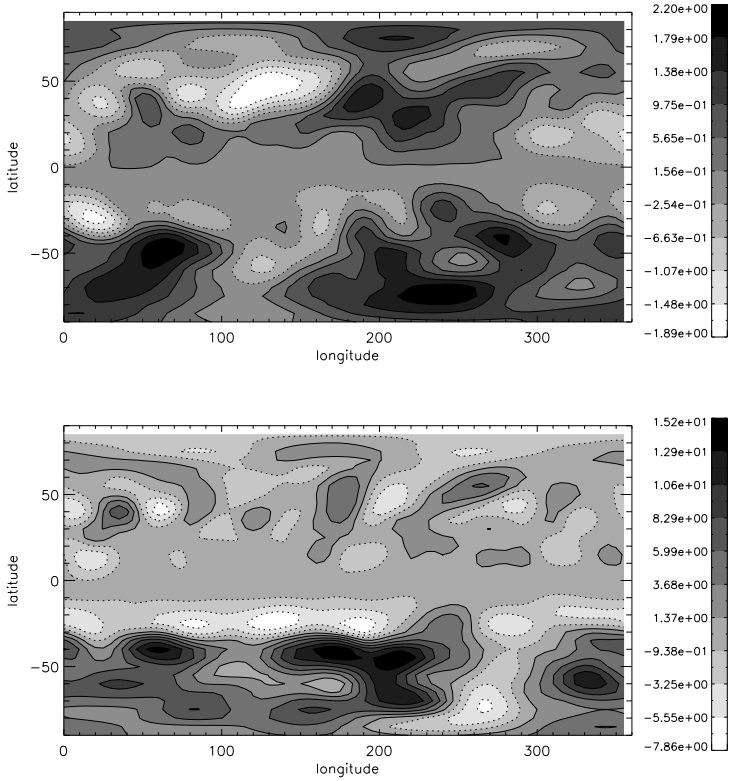

Figure: July temperature (top) and temperature forcing (bottom) anomalies in a two-level quasigeostrophic climate model of the periods 1949-1968 and 1975–1994.

Two-level quasigeostrophic potential vorticity equations

$$\frac{\partial q^j(t)}{\partial t} = -J\left[\psi^j(t), q^j(t)\right] - B\frac{\partial \psi^j(t)}{\partial \lambda} - d_0^j \zeta^j(t) + \kappa\left[\tilde{q}^j - q^j(t)\right]$$

where ψ^j is the streamfunction, ζ^j is the vorticity and q^j is the potential vorticity. $J[\psi^j, q^j]$ is the nonlinear adective term, B is the Coriolis parameter, and d_0^j is the dissipation operator. κ is the Newtonian relaxation. $\tilde{q}^j$ is the forcing function.

- How do we find $\tilde{q}^j$ that is consistent with the time averages $\langle q^j \rangle$ (also $\langle \psi^j \rangle$ and $\langle \zeta^j \rangle$) at statistical steady state?

Iterative method

$$
\begin{aligned}
\left[\tilde{q}^j\right]_0 &= \left\langle \left[q^j\right]_{obs} \right\rangle \\
\left[\tilde{q}^j\right]_i &= \left[\tilde{q}^j\right]_{i-1} + \left\langle \left[q^j\right]_{obs} \right\rangle - \left\langle \left[q^j\right]_{i-1} \right\rangle
\end{aligned}
$$

where i is the iteration step.

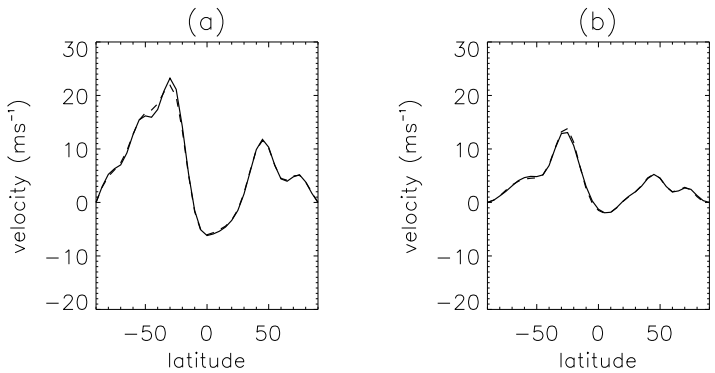

Figure: Climate simulation after 22 iterations (solid) compared to observed climate (dashed) for (a) barotropic and (b) baroclinic zonal wind.

Statistical dynamical method: Closure problem

General form of atmospheric spectral thermo-dynamical equations:

$$\begin{aligned}\frac{\partial x^j_{mn}}{\partial t} &= \sum_{pq}\sum_{rs}\sum_{kl}\left[\mathcal{K}^{jkl}(m,n;p,q;r,s)x^k_{-pq}x^l_{-rs} + \mathcal{A}^{jkl}(m,n;p,q;r,s)x^k_{-pq}\phi^l_{-rs}\right] \\ &- \sum_k D^{jk}_0(m,n)x^k_{mn} + f^j_0(m,n)\end{aligned}$$

Taking the time average at statistical steady state:

$$\begin{aligned}&\sum_{pq}\sum_{rs}\sum_{kl}\left[\mathcal{K}^{jkl}(m,n;p,q;r,s)\langle x^k_{-pq}\rangle\langle x^l_{-rs}\rangle + \mathcal{A}^{jkl}(m,n;p,q;r,s)\langle x^k_{-pq}\rangle\phi^l_{-rs}\right] \\ +\quad &\langle T^j_{mn}\rangle - \sum_k D^{jk}_0(m,n)\langle x^k_{mn}\rangle + \langle f^j_0(m,n)\rangle = 0,\end{aligned}$$

where

$$\langle T^j_{mn}\rangle = \sum_{pq}\sum_{rs}\sum_{kl}\mathcal{K}^{jkl}(m,n;p,q;r,s)\langle \hat{x}^k_{-pq}\hat{x}^l_{-rs}\rangle$$

and $\hat{x}^j_{mn} = x^j_{mn} - \langle x^j_{mn}\rangle$

Statistical dynamical method: Parameterisation

Parameterisation:

$$\langle T^j_{mn} \rangle = -\sum_k D^{jk}_t(m,n)\langle x^k_{mn} \rangle + f^j_t(m,n)$$

- Form motivated by the quasi-diagonal direct interaction approximation (QDIA) — an inhomogeneous statistical dynamical closure theory
- Ensemble of slightly different climates created
- $D^{jk}_t(m,n)$ and $f^j_t(m,n)$ calculated by least-squares linear regression

Statistical dynamical method: Closed form

The inverse climate model may then be written in the following way:

$$\sum_{pq}\sum_{rs}\sum_{kl}\left[\mathcal{K}^{jkl}(m,n;p,q;r,s)\langle x^k_{-pq}\rangle\langle x^l_{-rs}\rangle + \mathcal{A}^{jkl}(m,n;p,q;r,s)\langle x^k_{-pq}\rangle\phi^l_{-rs}\right]$$
$$- \quad \sum_k D^{jk}_r(m,n)\langle x^k_{mn}\rangle + \langle f^j_r(m,n)\rangle = 0,$$

where

$$D^{jk}_r(m,n) = D^{jk}_0(m,n) + D^{jk}_t(m,n)$$

and

$$\langle f^j_r(m,n)\rangle = \langle f^j_0(m,n)\rangle + f^j_t(m,n).$$

Results: Linear regression of ensemble data points (1)

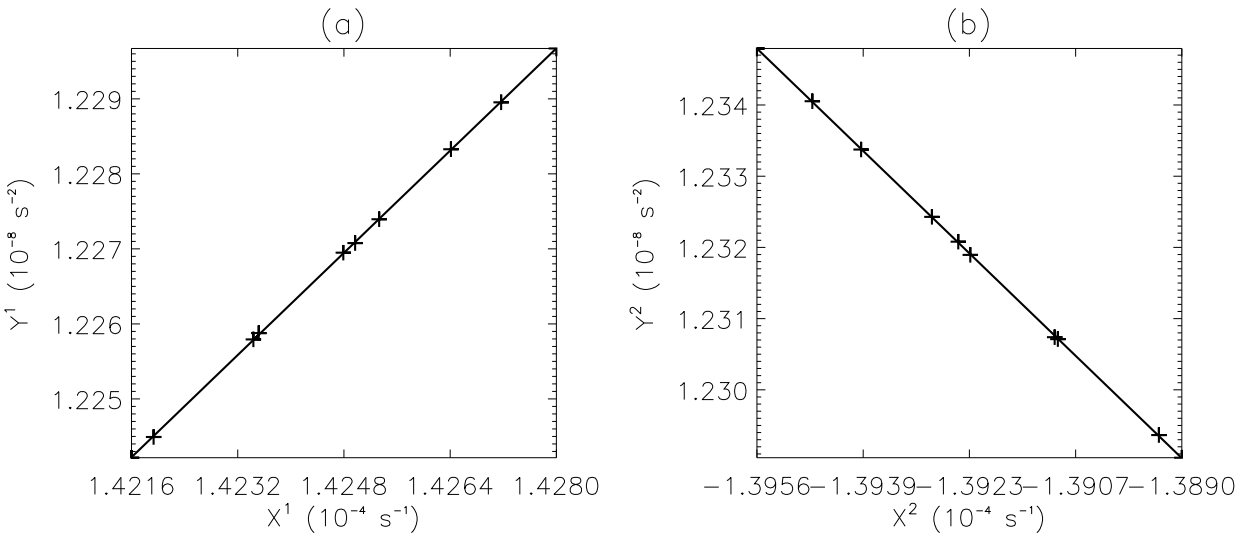

Figure: Variation of the mean nonlinear tendency with the mean potential vorticity for $m = 0$ and $n = 1$ for (a) Level 1 and b) Level 2. Here, $Y^1 = Re\{\langle T^1 \rangle + D^{12}\langle q^2 \rangle\} - Im\{D^{11}\}Im\{\langle q^1 \rangle\}$, $Y^2 = Re\{\langle T^2 \rangle + D^{21}\langle q^1 \rangle\} - Im\{D^{22}\}Im\{\langle q^2 \rangle\}$, $X^1 = Re\{\langle q^1 \rangle\}$, and $X^2 = Re\{\langle q^2 \rangle\}$. The straight line is obtained by linear regression.

Results: Linear regression of ensemble data points (2)

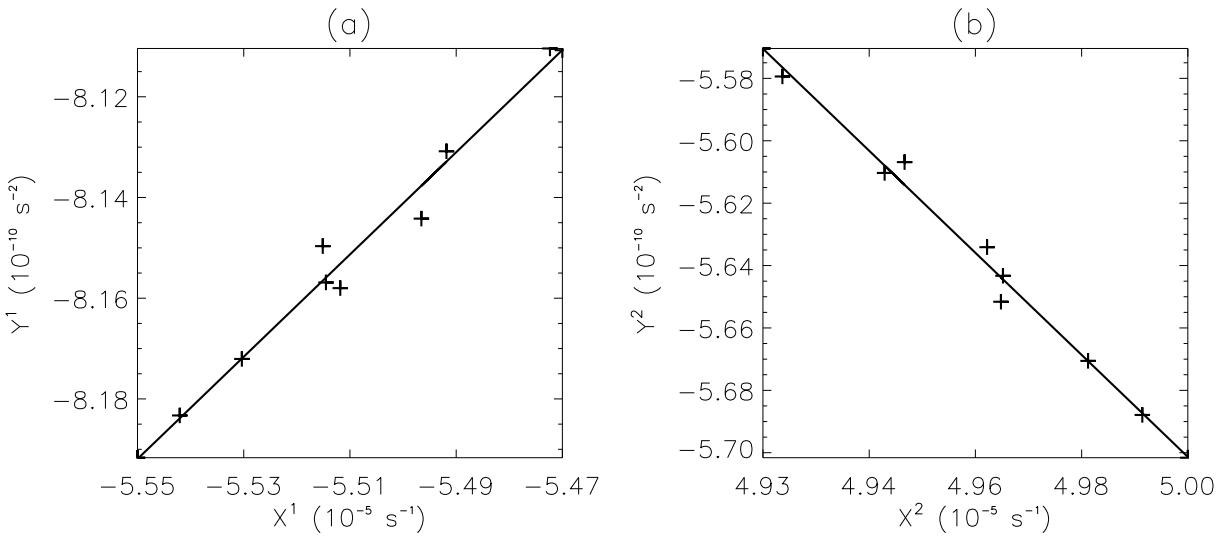

Figure: Variation of the mean nonlinear tendency with the mean potential vorticity for $m = 0$ and $n = 2$ for (a) Level 1 and b) Level 2. Here, $Y^1 = Re\{\langle T^1 \rangle + D^{12}\langle q^2 \rangle\} - Im\{D^{11}\}Im\{\langle q^1 \rangle\}$, $Y^2 = Re\{\langle T^2 \rangle + D^{21}\langle q^1 \rangle\} - Im\{D^{22}\}Im\{\langle q^2 \rangle\}$, $X^1 = Re\{\langle q^1 \rangle\}$, and $X^2 = Re\{\langle q^2 \rangle\}$. The straight line is obtained by linear regression.

Results: Forcing function anomalies compared

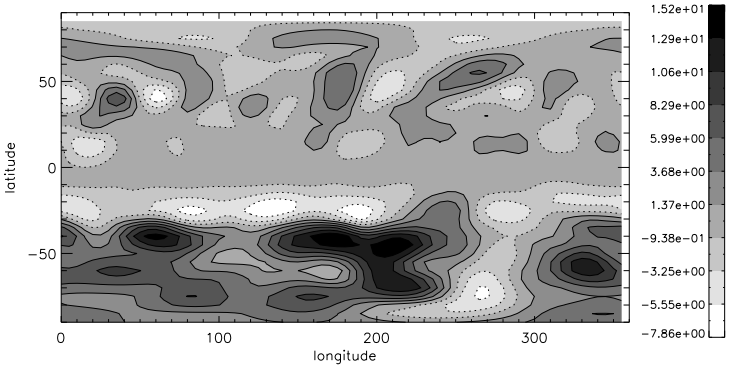

Figure: Anomalies of the temperature forcing function (scaled by κ^{-1}) in the July 1975–1994 and July 1949–1968 climate simulations (calculated iteratively)

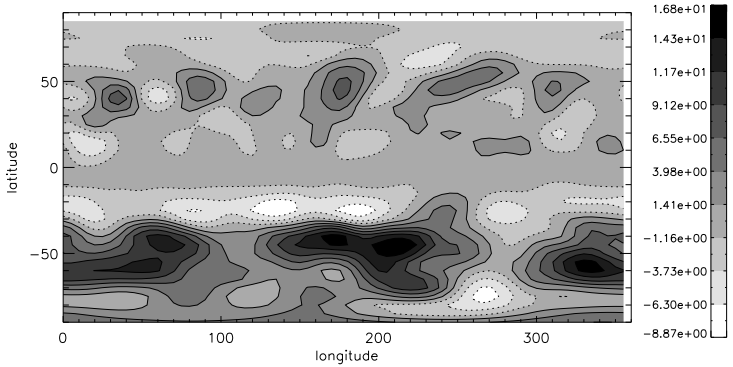

Figure: Anomalies of the temperature forcing function (scaled by κ^{-1}) in the July 1975–1994 and July 1949–1968 climate simulations (calculated by linear regression)

Summary and Conclusion

- Changes in southern hemisphere winter circulation (related to changes in storm tracks) can be simulated by climate models with appropriate Greenhouse forcing
- Changes in circulation and storm tracks are enhanced under different emission scenarios in the 21st Century
- Climate forcing can be calculated iteratively from climate data
- Climate forcing can also be calculated more efficiently using a statistical dynamical method
- Climate forcing calculated by statistical dynamical method in good agreement with that calculated iteratively
- Anomalous forcing functions calculated by both methods reveal a tendency towards low latitude cooling and high latitude heating

References

- Frederiksen, J.S. and Frederiksen, C.S. 2007. Inter-decadal changes in Southern Hemisphere winter storm track modes. Tellus, 59A, 559–617.
- Frederiksen, C.S., Frederiksen, J.S., Sisson, J.M., and Osbrough, S.L. 2011. Australian winter circulation and rainfall changes and projections. International Journal of Climate Change Strategies and Management, Paper 4, Vol. 3, Issue 2.
- Zidikheri, M.J. and Frederiksen, J.S. Inverse method for attribution of climate change. Submitted to ANZIAM Journal.